Journal of Fundamental and Applied Sciences

Research Article

ISSN 1112-9867

Available online at http://www.jfas.info

NON-LINEAR BACKSTEPPING SPEED CONTROL FOR ASIAN ELECTRIC SCOOTER USES

H. Chergui[1], A. Nasri[1,*] K. Korhan[2]

[1]Laboratory of Smart Grids & Renewable Energies (S.G.R.E), Faculty of Technology, Department of Electrical Engineering, Tahri Mohamed University Bechar, B.P 417, 08000, Algeria

[2]Department of Electric Electronics, Faculty of Engineering, Nisantasi University, 34310, Istanbul, Turkey

Received: 01 October 2020 / Accepted: 08 November 2020 / Published online: 01 January 2021

ABSTRACT

The electric scooter has become very popular especially in large European and Asian urban areas, thanks to its some advantages. While its popularity is increasing, studies about these electric scooters are also increasing. The main objective of this study is to introduce the design of an autonomy extended electric three-wheeled scooter. For this aim, a model is obtained firstly and it is driven by two BLDC motors placed on the rear wheels independently controlled by a non-linear controller named as Backstepping. Indeed, it contains a powerful electronic differential system to ensure the security of passenger while entering the curved road. The studied model is simulated through the MATLAB Simulink environment where interesting results are shown in results.

Keywords: Electric scooter; Electronic differential; BLDCM; Backstepping controller.

Author Correspondence, e-mail: nasriab1978@yahoo.fr

doi: http://dx.doi.org/10.4314/jfas.v13i1.21

1. INTRODUCTION

In the past, private cars were considered as luxury, however today they are becoming more popular and a requirement. Moreover, most people view them as essential to their lives. One of the biggest problems facing the world due to increase of usage is the waste of non-renewable energy where the preservation of these resources have become a priority. On the other hand, a more serious problem emerges as car engines CO2 emissions, which left off the biggest environmental problems of pollution and global warming.

Owing to the enormous density of vehicles, there are always traffic jams in major cities, also causing production cessation and may be sometimes it can be a dangerous factor to human life. It is possible that there are currently thousands of people stranded on the roads around or without power [1].

Though the progress of research and the shift to electric vehicles as a solution to the problem for land transportation, it is still difficult to be achieved because of high-density storage systems, except in the case of lightweight vehicles such as motorcycles and electric scooter.

Electric scooters have become popular in many large urban areas especially in Asian cities because of its advantages among them: easy to move in the city, does not produce any harmful gases to the environment, low noise, great independence, lack of energy consumption because of the engine does not exceed in general 3000w and the scooter’s small size which provides more space on the roads [2].

Previous studies show that generally PMSM or BLDC motors are used in electric scooters. Also, there are some studies about backstepping control algorithm for PMSM and BLDC motors. In a study, a research about backstepping high order sliding mode control was performed for servo system speed control [3]. An adaptive backstepping control of PMSM was studied with modelling and simulation [4]. In another studies, an adaptive integrator backstepping tracking controller for BLDC motor, backstepping control to AC position servo system, sliding mode control with backstepping in BLDC motor servo system and backstepping controller modelling for position servo controller of PMSM were investigated [5-8]. On the other hand, there are some researches about hybrid recurrent wavelet neural network control of PMSM used in an electric scooter, adaptive power split control for a hybrid electric scooter, adaptive Legendre

neural network control for PMSM servo drive electric scooter were studied [9-11]. Additionally, in another study, fuzzy sliding mode control was used to traction control for electric scooter. Road friction coefficient was estimated by using double observer for direct driven wheel motor [12]. In another study, a torque control algorithm was implemented for BLDC motor applied to electric vehicles and it was performed experimentally with using TMS320F240 dsp [13]. Adaptive neural network method was used to control of a self balancing two wheeled scooter with differential driving and two dc motors is used for this application [14]. For two-wheel electric scooter, an adaptive backstepping self-balancing controller was performed by Son N.N et al. and in another paper, hybrid PD and adaptive backstepping control for self-balancing two-wheel electric scooter was studied [15-16].

This paper deals with a model of an electric scooter with two BLDC motors placed on the rear wheels is independently controlled by a non-linear backstepping controller. The electronic differential system of the electric scooter provides powerful control when it enters a curvy road. The modeling and simulation of this system is applied and compared in the MATLAB Simulink environment, with the same system whose speed is controlled by a classic pi controller

The first section of this paper deals with the general description of the traction system. The next section presents the mathematical model of the engine and the speed control unit. The third section presents the mathematical equations that represent the force applied to the system as well as the mathematical equations of the electronic differentiators. Section four exposes the results of simulation and the last section is a conclusion.

2. COMPONENTS AND MODELS OF ELECTRIC SCOOTER

A general schematic diagram of an electric scooter traction system that consists of a BLDC motor controlled by a voltage inverter supplied by a lithium battery terminal is shown in Fig.1 [1].

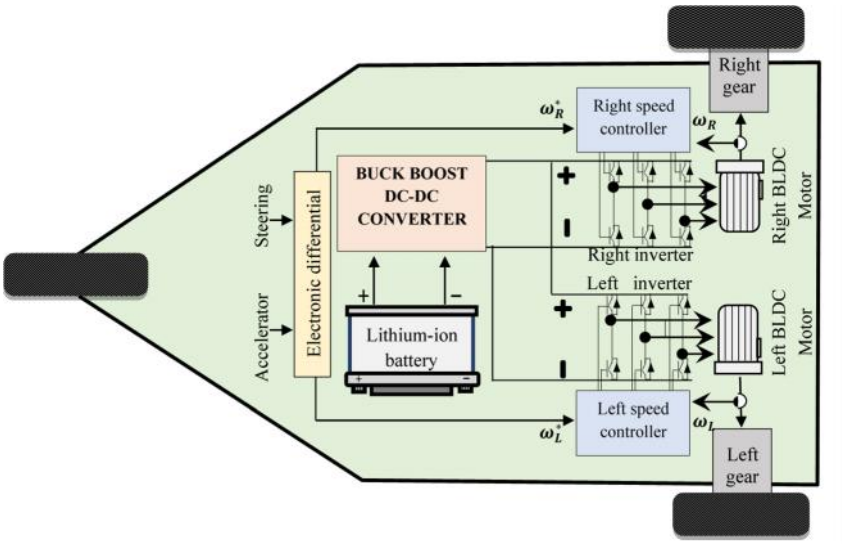

Fig.1. Block diagram of the proposed system

2.1. Storage system

The lithium battery is widely used especially in the light electric vehicles, electric motorcycles and electric scooters because of its advantages, more precisely the high density compared to light weight [17].

There are two situations of lithium battery as charge and discharge. The equations of these situations for the lithium battery are given in Eq.1 and Eq.2.

For if > 0 (Discharge model)

$$f_{dis}(i_c, i_f) = E_0 - \frac{k \cdot Q_M}{Q_M + i_c} i_f - \frac{k \cdot Q_M}{Q_M - i_c} i_c + \sim e^{-\ i_c} \tag{1}$$

For if < 0 (Charge model)

$$f_{dis}(i_c, i_f) = E_0 - \frac{k \cdot Q_M}{0.1 \cdot Q_M + i_c} i_f - \frac{k \cdot Q_M}{Q_M - i_c} i_c + \sim e^{-\ i_c} \tag{2}$$

In the equations, E0 is constant voltage (V), k is steady constant (Ah), if is low frequency current dynamics (A), ic is extorted capacity (Ah), QM is maximum battery capacity (Ah), α is exponential voltage (V), β is exponential capacity (Ah) [17].

The state of charge (SOC) is calculated with the following equation [21]:

$$SOC = 100(1 - \frac{1}{Q_M} \int_0^t i(t)dt) \tag{3}$$

2.2. DC-DC Buck-boost converter

The buck-boost converter is a type of DC-DC converter in which the output voltage value can

be greater than or smaller than the input voltage depending on the duty cycle [18]. The operating principle of this converter is that the inductor is not allow sudden variations in input current. Inductor stores energy when power switch is on state. When the power switch is off state, it discharges. These two situations depend on power switch provides buck-boost structure. By the help of the capacitor, the converter circuit supply a constant output voltage. The output voltage is depending on duty cycle and can be obtained with the Eq.4. Where, D is duty cycle.

$$V_{out} = V_{in}\frac{D}{1-D} \tag{4}$$

The PI controller is integrated into the Buck-Boost Converter to adjust the duty cycle so as to make the output voltage direct and constant whatever the value of the applied load. Its Buck-Boost Converter circuit and its controller are shown in Fig. 2 [19].

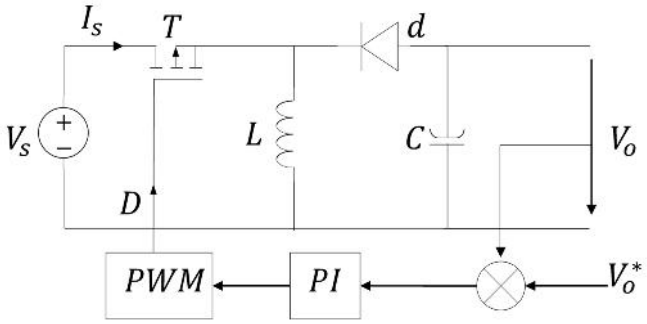

Fig.2. A classical buck-boost converter circuit

2.3. Mathematical model of the BLDCM

Suppose the magnetic circuit is unsaturated and the hysteresis and eddy current losses are ignored. The mathematical model of a conventional surface mounted BLDCM can be given with the standard assumptions above in the d – q [20, 22-23]:

$$\frac{di_d}{dt} = -\frac{R}{L}i_d + p\mu i_q + \frac{1}{L}u_d \tag{5}$$

$$\frac{di_q}{dt} = -\frac{R}{L}i_q + p\mu i_d - \frac{p¤_f}{L}\mu + \frac{1}{L}u_d \tag{6}$$

$$\frac{d\mu}{dt} = \frac{3p¤_f}{2j}i_q - \frac{B}{j}\mu - \frac{1}{j}T_L \tag{7}$$

Where, L is stator inductances and R is the stator resistance, *id*, *iq* are the d-axes and q-axes stator currents, *ud*, *uq* denote the d-axes and q-axes stator voltages, *p* is the number of pole pairs of the BLDC motor, ω is the rotor angular speed of the motor, ϕf is the flux linkage, *TL*

represents the load torque, *j* is the rotor inertia and *B* is the viscous friction coefficient.

2.4. Design of Backstepping controller

The backstepping control design consists of two main designs [23]. These controllers are presented in two parts as:

- Speed controller design
- Current controller design

Speed controller design

The design of the speed controller consists of three steps. First step is e_1 variable error tracking status, second step is obtain μ^* the reference rotor angular speed of the motor and third step is deriving of the Lyapunov functions.

Step 1: To track speed, the e_1 variable error tracking status can be defined as*:*

$$e_1 = \mu^* - \mu \tag{8}$$

Where, μ^* is the reference rotor angular speed of the motor. After derivation,

$$\dot{e}_1 = \dot{\mu}^* - \dot{\mu} \tag{9}$$

$$\dot{e}_1 = \frac{1}{j}(B\mu + T_L - \frac{3p¤_f}{2} i_q) \tag{10}$$

Step 2: The Lyapunov function is defined as follows*:*

$$V_1 = \frac{1}{2} e_1^2 \tag{11}$$

Step 3: Deriving of the Lyapunov function gives:

$$\dot{V}_1 = e_1 \dot{e}_1 \tag{12}$$

$$\dot{V}_1 = \frac{e_1}{j}(B\mu + T_L - \frac{3p¤_f}{2} i_q) \tag{13}$$

The Lyapunov stability definition allows for error tracking to be converged to 0 in the saturation status as it must be $\dot{V}_1 < 0$.

$$\frac{1}{j}(B\mu + T_L - \frac{3p¤_f}{2} i_q) = -k_1 e_1, \_ k_1 > 0 \tag{14}$$

Through the nonlinear Backstepping method in Eq.14, we obtain the value of i_q reference as shown in Eq.15,

$$i_{qref} = \frac{2}{3p¤_f}(k_1 je_1 + B\mu + T_L) \tag{15}$$

Through the above equations we can get,

$$\dot{V}_1 = -k_1 \dot{e}_1^2 \tag{16}$$

Current controller design

Step 1: To track the proposed i_q, the new e_2 variable error tracking status can be defined as*:*

$$e_2 = i_q^* - i_q \tag{17}$$

The derivation of e_2 gives us:

$$\dot{e}_2 = \dot{i}_q^* - \dot{i}_q \tag{18}$$

$$\dot{e}_2 = \frac{2(B - k_1 j)}{3p¤_f j}\left(\frac{3p¤_f}{2} i_q - B\mu - T_L\right) + \frac{R}{L} i_q + p\mu i_d - \frac{u_q}{L} + \frac{p¤_f}{L}\mu \tag{19}$$

Step 02: The second Lyapunov function is defined as follows*:*

$$V_2 = V_1 + \frac{1}{2} e_2^2 \tag{20}$$

Step 03: Derivation of a second function for Lyapunov is given as,

$$\dot{V}_2 = \dot{V}_1 + e_2 \dot{e}_2 \tag{21}$$

$$\dot{V}_2 = -k_1 e_1^2 + e_2\left[\frac{2(B - k_1 j)}{3p¤_f j}\left(\frac{3p¤_f}{2} i_q - B\mu - T_L\right) + \frac{R}{L} i_q + p\mu i_d - \frac{u_q}{L} + \frac{p¤_f}{L}\mu\right] \tag{22}$$

The Lyapunov stability definition allows for error tracking to be converged to zero in the saturation status, as it must be $\dot{V}_2 < 0$.

$$\frac{2(B - k_1 j)}{3p¤_f j}\left(\frac{3p¤_f}{2} i_q - B\mu - T_L\right) + \frac{R}{L} i_q + p\mu i_d - \frac{u_q}{L} + \frac{p¤_f}{L}\mu = -k_2 e_2, \_ k_2 > 0 \tag{23}$$

Through the nonlinear Backstepping method in Eq.23, the value of u_q is given as:

$$u_q = L\left[\frac{2(B - k_1 j)}{3p¤_f j}\left(\frac{3p¤_f}{2} i_q - B\mu - T_L\right) + \frac{R}{L} i_q + p\mu i_d + k_2 e_e + \frac{p¤_f}{L}\mu\right] \tag{24}$$

Through the above functions, we can get:

$$\dot{V}_2 = -k_1\dot{e}_1^2 - k_2\dot{e}_2 \tag{25}$$

In the same method: i_d's design consists of the following steps*:*

Step 1: To track the proposed i_d, the error tracing status of the new variable e_3 can be defined as*:*

$$e_3 = i_d^* - i_d \tag{26}$$

$$\dot{V}_3 = -k_1\dot{e}_1^2 - k_2\dot{e}_2^2 - k_3\dot{e}_3^2 \tag{27}$$

The derivation of e_3 gives us

$$\dot{e}_3 = \dot{i}_d^* - \dot{i}_d \tag{28}$$

Where idref=0

Step 2: The third function of Lyapunov is defined as follows:

$$V_3 = V_2 + \frac{1}{2}e_3^2 \tag{29}$$

Step 3: The Derivation of a third function for Lyapunov gives*:*

$$\dot{V}_3 = \dot{V}_2 + e_3\dot{e}_3 \tag{30}$$

$$\dot{V}_3 = -k_1e_1 - k_2e_2 + e_3(\frac{R}{L}i_d - p\mu i_q - \frac{u_d}{L}) \tag{31}$$

Where $\dot{V}_3 < 0$.

$$\frac{R}{L}i_d - p\mu i_q - \frac{u_d}{L} = -k_3e_3, \_ k_3 > 0 \tag{32}$$

Through the nonlinear Backstepping method in Eq.32, the value of ud is given as*:*

$$u_d = Ri_d - pL\mu i_q + Lk_3e_3 \tag{33}$$

Through the above functions, we can get:

$$\dot{e}_3 = \frac{R}{L}i_d - p\mu i_q - \frac{u_d}{L} \tag{34}$$

From the above equations, we can observe that the function of Lyapunov V3>0 and derivative $\dot{V}_3 < 0$ indicates that the error trace is converged to 0. The block diagram of the BLDCM whell

speed control system is shown in Fig.3.

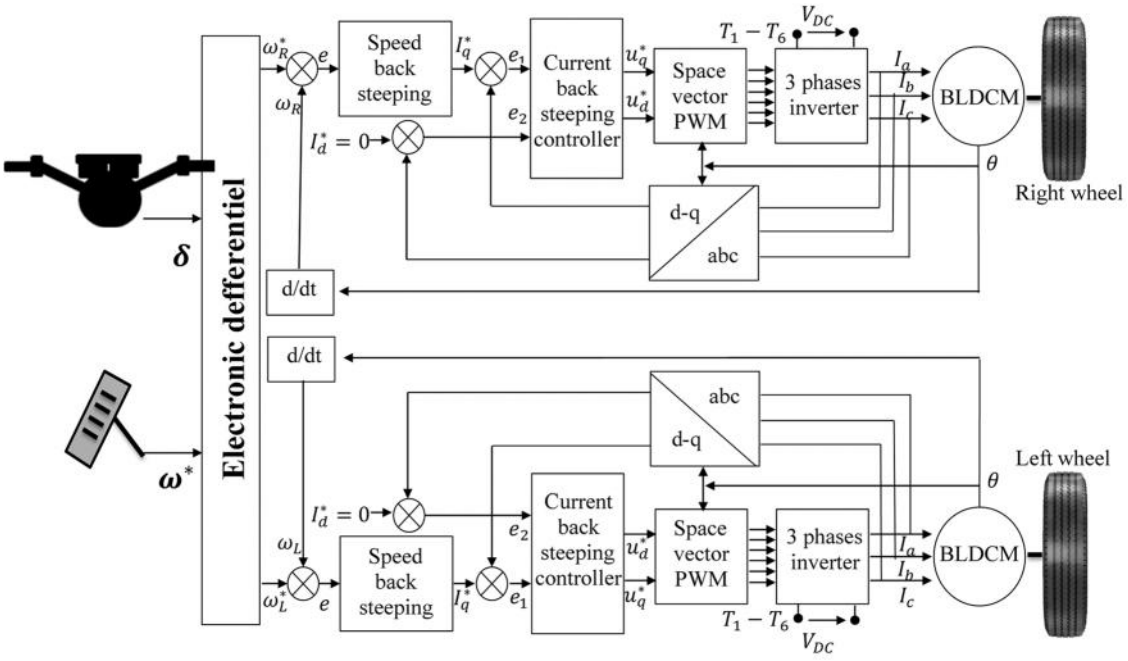

Fig.3. Block diagram of the BLDCM wheel speed control system

3. PERFORMANCE OF ELECTRIC SCOOTER UNDER LOAD

The resistance forces applied to the scooter while traversing a road is shown in Fig.4.

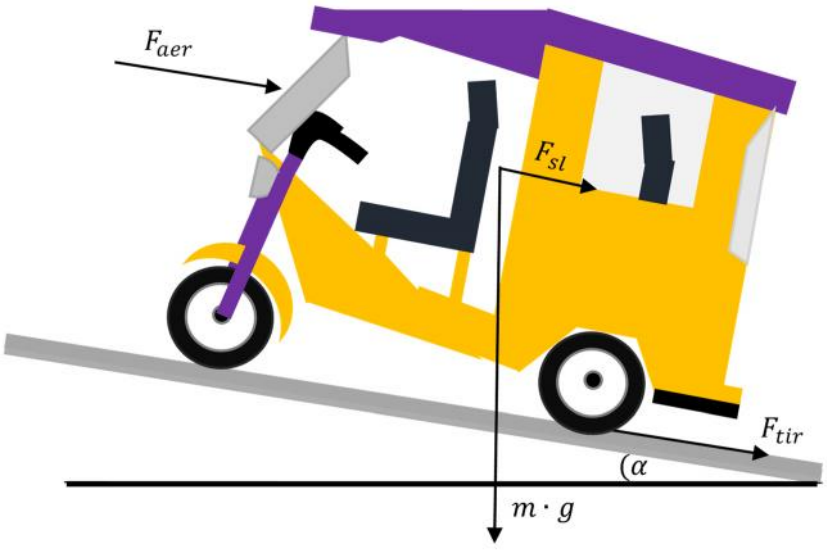

Fig .4. The electric scooter acting forces during road

Additionally, the sum of the resistance forces applied to the electric scooter can be summarized

as follows [18]:

$$F_r = F_{tir} + F_{aer} + F_{sl} \tag{35}$$

The rolling resistance force Ftir is defined by:

$$F_{tir} = f_r \cdot m \cdot g \tag{36}$$

The aerodynamic resistance torque Faer is given as:

$$F_{aer} = \frac{1}{2} \cdot \circ_a \cdot s \cdot c_x \cdot V_L^2 \tag{37}$$

The slope resistance force Fsl is usually modelled as:

$$F_{sl} = m \cdot g \cdot \sin \sim \tag{38}$$

Where, m is the scooter mass, fr is the rolling resistance force constant, g the gravity acceleration, ρα is the air density, cx is the aerodynamic drag coefficient, s is the frontal surface area of the vehicle.

3.1. Electronic Differentials

When the scooter starts on a straight road, all wheels get the same speed. But when entering a curved road, the outer wheels became faster than the inner wheels. Here comes the role of electronic differentials to give each engine the necessary speed to maintain the stability of the vehicle starting from the dimensions of the vehicle and the radius of the turn and the angle of rotation [1], as shown in Fig.5.

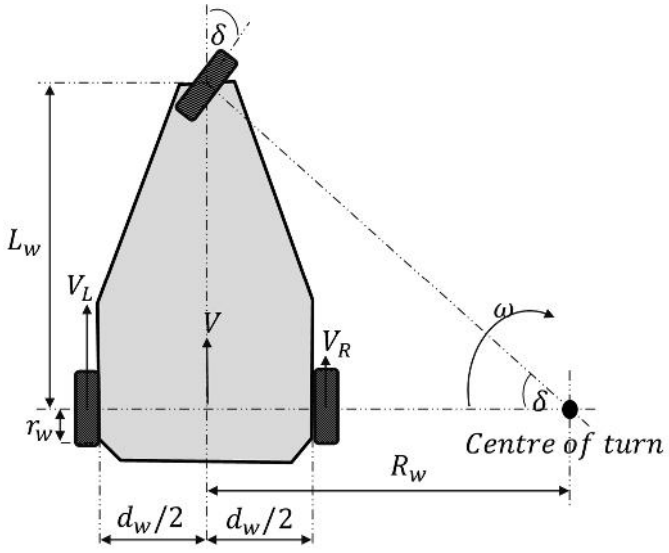

Fig.5. The electric scooter moving on curved road

The proportionality between the speed and distance from the center of the bend is given by the following equation:

$$\frac{V^*}{R_w} = \frac{V_R^*}{R_w - d_w/2} = \frac{V_L^*}{R_w + d_w/2} \tag{39}$$

V_R^* and V_L^* are expressed by the following equations:

$$\begin{cases} V_R^* = V^*(\dfrac{R_w - d_w/2}{R_w}) \\ V_L^* = V^*(\dfrac{R_w + d_w/2}{R_w}) \end{cases} \tag{40}$$

$$\begin{cases} V_R^* = V^*(1 - \dfrac{d_w}{2R_w}) \\ V_L^* = V^*(1 + \dfrac{d_w}{2R_w}) \end{cases} \tag{41}$$

Where:

$$R_w = \frac{L_w}{\tan(¢)} \tag{42}$$

From equation 41 and 42 we get :

$$\begin{cases} V_R^* = V^*(1 - \dfrac{d_w \tan(¢)}{2L_w}) \\ V_L^* = V^*(1 + \dfrac{d_w \tan(¢)}{2L_w}) \end{cases} \tag{43}$$

$$\begin{cases} V_R^* = V^* - \Delta V \\ V_L^* = V^* + \Delta V \end{cases} \tag{44}$$

The distinction between traction wheel linear speeds is:

$$\Delta V = \frac{d_w \tan(¢)}{2L_w} V^* \tag{45}$$

Where, R_w, L_w, d_w and $¢$ are rotating radius, wheelbase, distance between driving wheels and steering angle, respectively.

The speed change is being changed with adding and subtracting to/from the average value of the wheels' reference speed (V^*) to obtain each reference back linear speed (V_R^* , V_L^*). In the Eq.45, $¢$ is also used for determining the trajectory. When the value of $¢$ is lower than zero

($¢ < 0$), it turns left. If $¢$ is equal to zero ($¢ = 0$), go straight. And the other situation, when the value of $¢$ is higher than zero ($¢ > 0$), it turns right [1].

4. RESULTS

The system is simulated in the MATLAB Simulink environment, and the results are presented in four tips*:*

- The scooter (the mechanical side)
- The motor
- DC-DC back boost converter
- The battery

4.1 The Scooter

The proposed model is simulated at different speeds under various conditions across the topography of a road as shown in Fig.6 and Table 1.

Table 1. The studied road topology

Time (s)	Phase number	Speed (km/h)	Description
[0:5]	1	20	straight road topology
[5:10]	2	40	straight road
[10:15]	3	40	Right curved road
[15:20]	4	40	straight road driving
[20:25]	5	40	the scooter moving on slope road
[25:30]	6	40	straight road

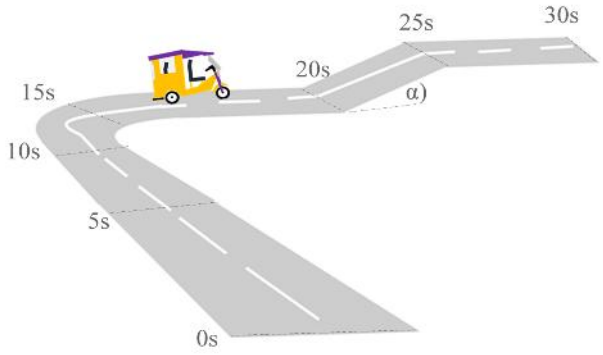

Fig. 6. The natural driving road topology

Figure 6 presents the phases that the scooter travels through in the case of a straight road. Here,

all the wheels get the same speed, but when entering a bend, the outer wheels become faster than the inner wheels. Figure 7 and 8 show both the wheel speed of rear and the zoomed wheel speeds of rear, respectively.

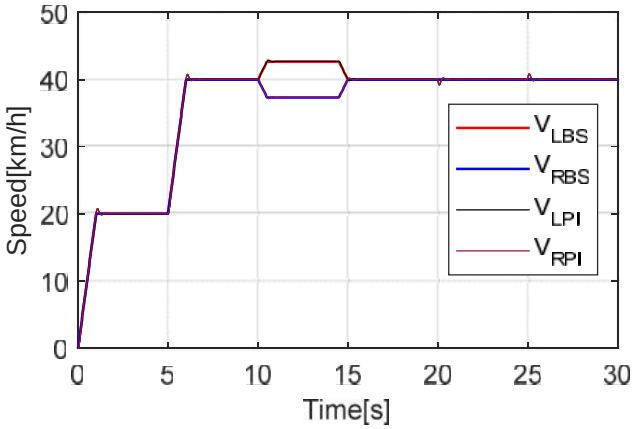

Fig.7. Wheel speeds of rear

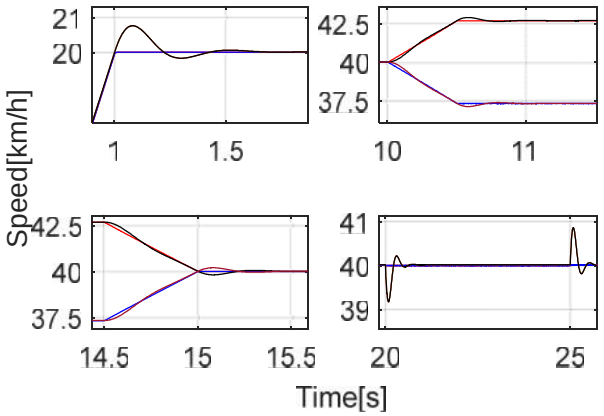

Fig.8. Zoomed wheel speeds of rear

The obtained results are presented with comparison of the nonlinear controller with the classical controller as shown in Figure 8. The high efficiency of the non-linear controller in controlling the speed under different road conditions is obtained.

Table 2. Performances of the PI and Backstepping controller for the speed response

Controller	Rising Time[s]	Settling Time [s]	Overshooting [%]
PI Controller	0.2541	0.4136	2.50
Backstepping Controller	0.1125	0.1333	0.002

Table 2 shows the high efficiency of non-linear controller by minimizing the three indicators (stabilization time, rise time and overflow limit) and it is compared with the classic PI controller. Figures 9 ,10, 11 and 12 show the scooter resistive torques, the aerodynamic torque of the scooter, the scooter total resistive torques and travelled distance, respectively.

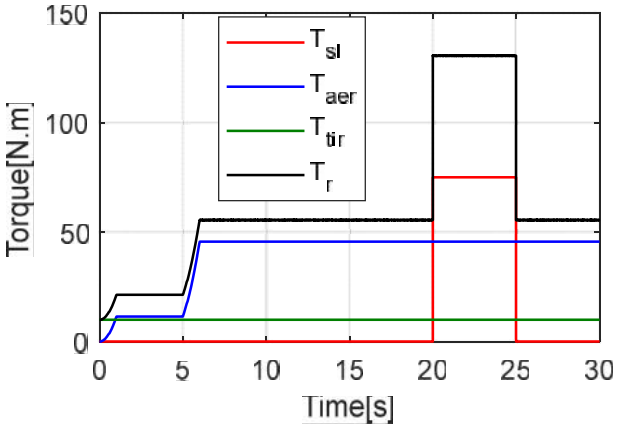

Fig.9. The scooter resistive torques

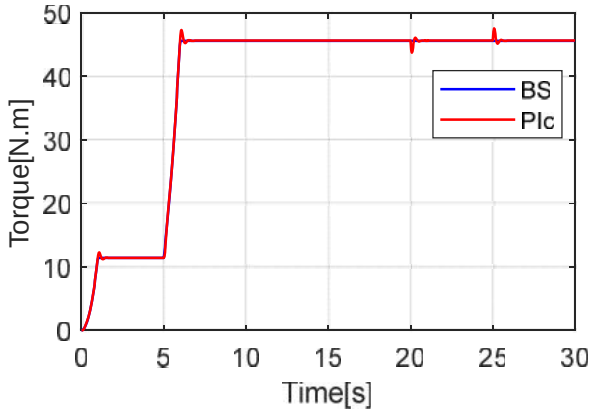

Fig.10. Aerodynamic torque of the scooter

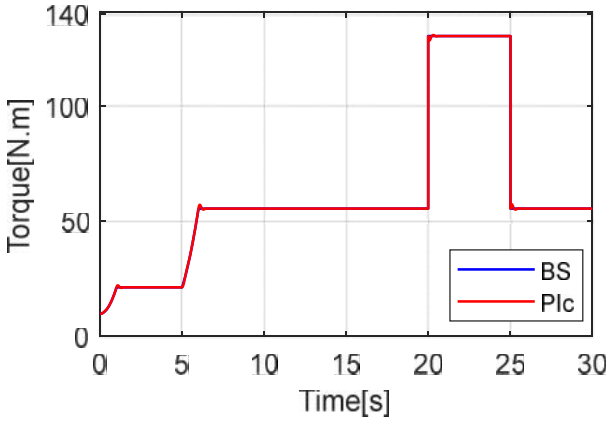

Fig.11. Scooter total resistive torques

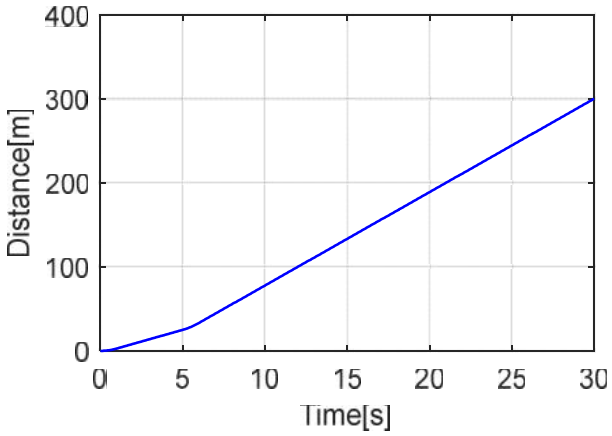

Fig.12. Travelled distance

The speed of electric scooter starts from 0km/h to 20km/h, which causes a load of up to 21.3Nm. In the second, third and fourth stages, the scooter runs at a speed of 40km/h, causing the application of a total torque on the system up to 55Nm. In the fifth phase, the total torque resistor applied to the system reaches over 130Nm due to entering a slope. Aerodynamic torque of the scooter and scooter total resistive torques are shown in Figure10 and Figure11, respectively. The aerodynamic torque, in the case of the application of the non-linear control unit on the system, became relatively lower compared with the application of the PI controller and shown in Table 3.

Table 3. Values of the aerodynamic torque and scooter resistive torque in different phases

Time [s]	**Aerodynamics Torque Taer [N.m]**		**Scooter resistive Torque T_r [N.m]**	
	PI	Backstepping	PI	Backstepping
1.08	12.28	11.4	22.18	21.29
6.08	47.28	45.58	57.17	55.48
20.08	43.69	45.57	128.6	130.5
25.08	47.56	45.58	57.45	55.48

The electric scooter crosses about 300m in 30 seconds as shown in Fig.12.

4.2 The BLDC motor

The results of the BLDC motor are presented in two parts (mechanical and electrical). Figure 13 and 14 present the BLDC motors angular speeds and the electromagnetic torques of the BLDC motors, respectively. They represent the results of the engine mechanical part.

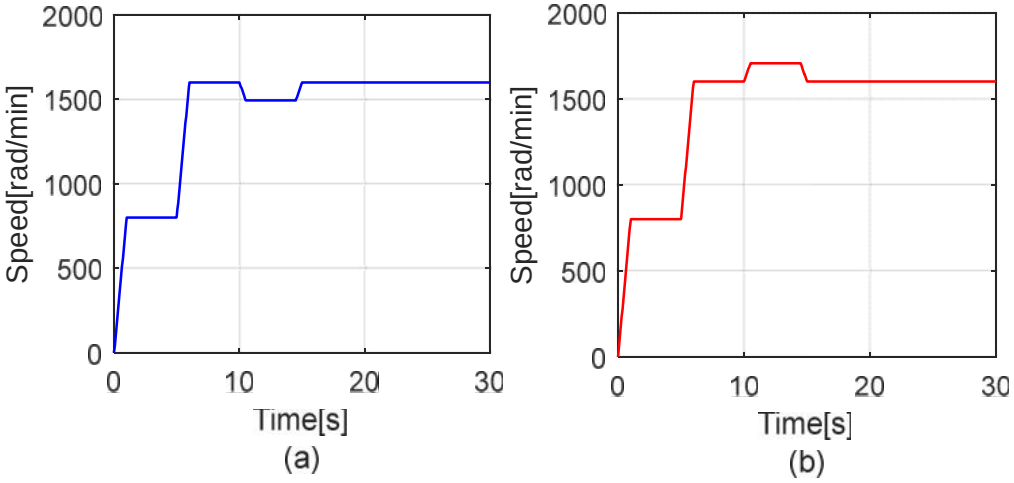

Fig.13. BLDC motors angular speeds ((a): right motor, (b): left motor)

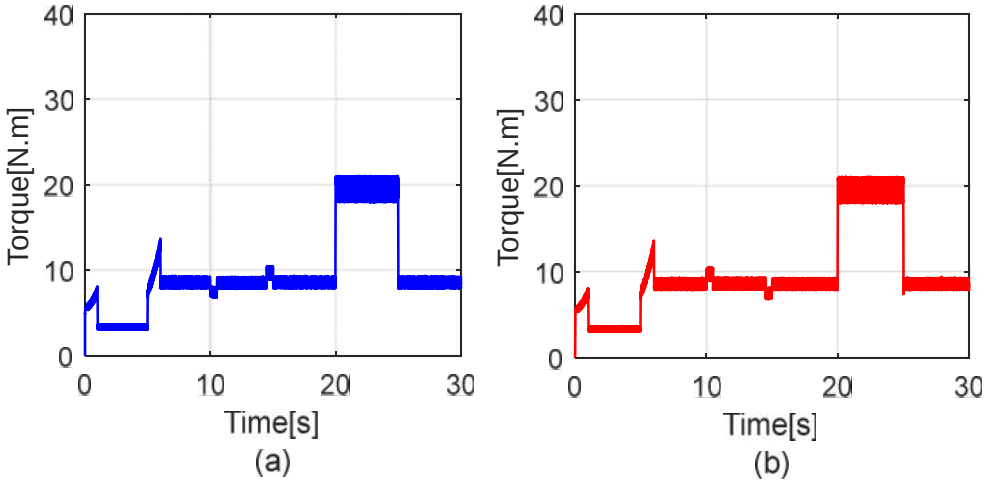

Fig.14. Electromagnetic torques of the BLDCM((a): rightmotor, (b): left motor)

When the acceleration is greater than zero, or if a torque load is applied, the electromagnetic torques of the motor increase. Figures 15 and 16, demonstrate the current of phase a and phase a back electromotive force of BLDC motor, respectively. These figures represent the results of the electric part of the motor. Here, it is noticeable that the increase in the electromagnetic torque has a direct effect on the increase in the current phases of this motor.

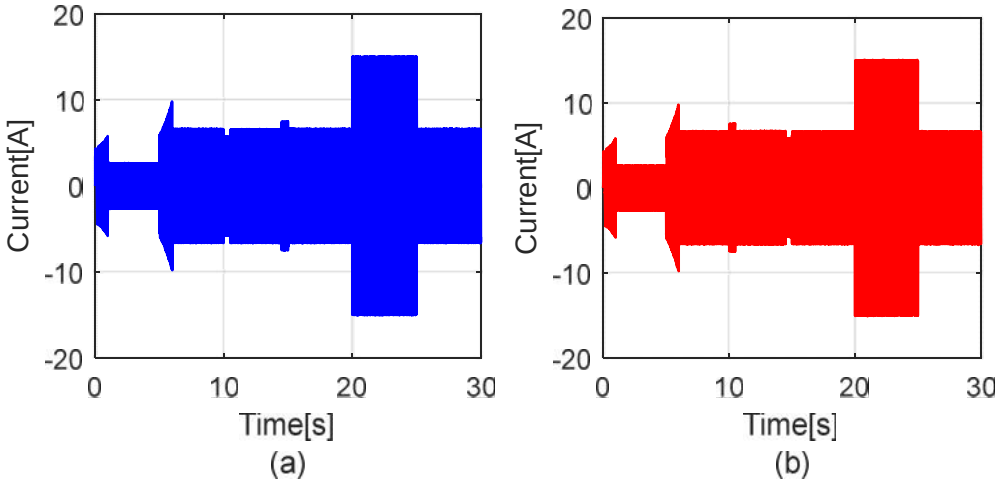

Fig.15. The current of phase a((a): right motor, (b): left motor)

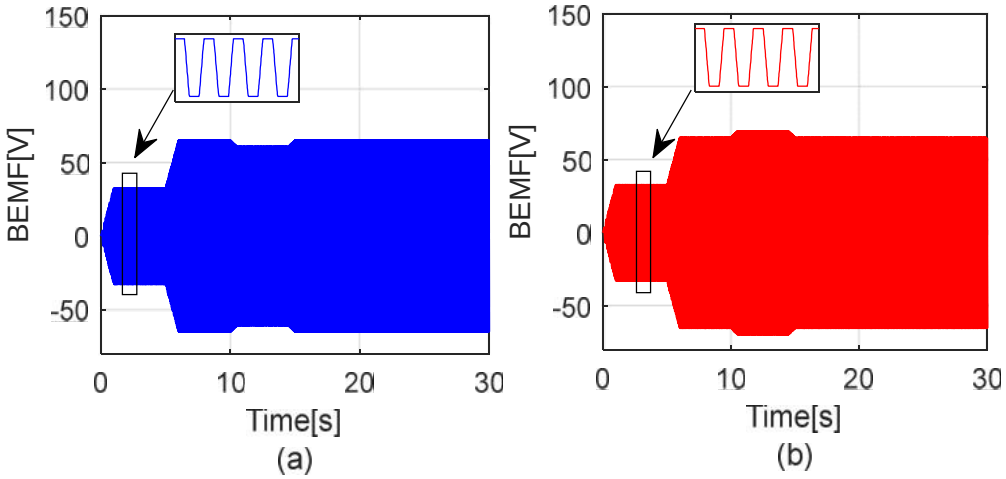

Fig.16. Phase a back electromotive force of BLDCM((a): right motor, (b): left motor)

4.3 The Buck-boost DC-DC converter

This part presents the results for the buck-boost DC-DC converter. Figure 17 shows the output voltage of buck-boost converter. In spite of the change in the current demand by the two motors, the buck-boost DC-DC converter provided good results because of the controller that kept the output voltage constant.

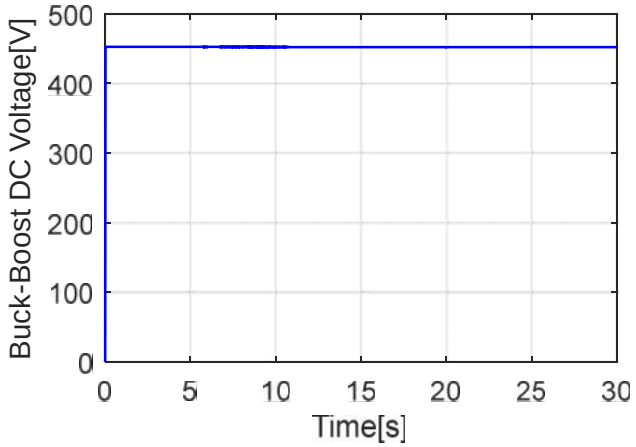

Fig.17. Output voltage of buck-boost converter

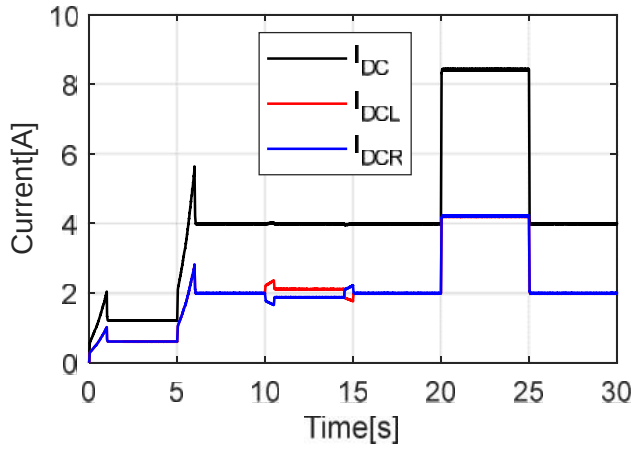

Fig.18. Output current of buck-boost converter

Figure 18 presents an output current of buck-boost converter where I_{DC} is load side current of the buck-boost converter, I_{DCR} is the input current for the right motor reflector and I_{DCL} is the input current for the left motor reflector.

4.4 The battery

Subjecting the scooter to different conditions (load and speed) led to notice an interesting result concerning the battery.

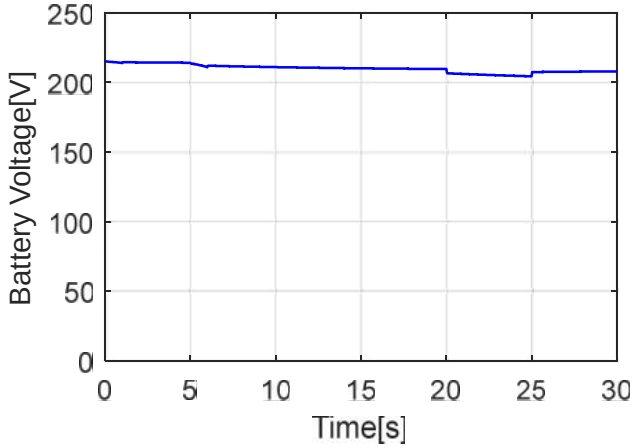

Fig.19. Battery output voltage

Figure 19 presents the battery output voltage where a slight change in noticeable in the output voltage due to the change in current demand during the different phases of this experiment. Figures 20 and 21 represent the battery current and the battery power, respectively when the system undergoes various disturbances. The state of the battery charge is shown in Fig.22.

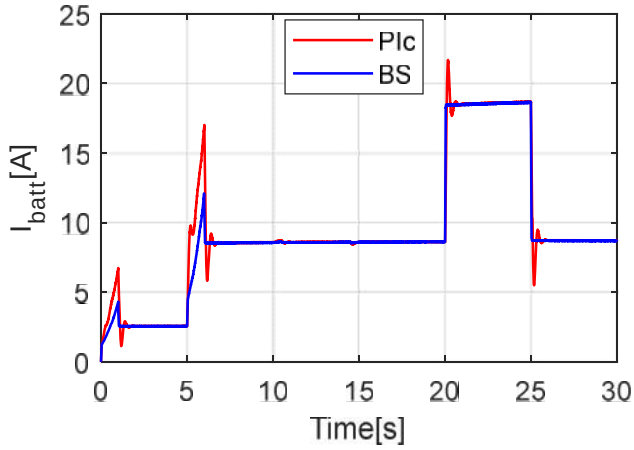

Fig.20. Battery current in different cases

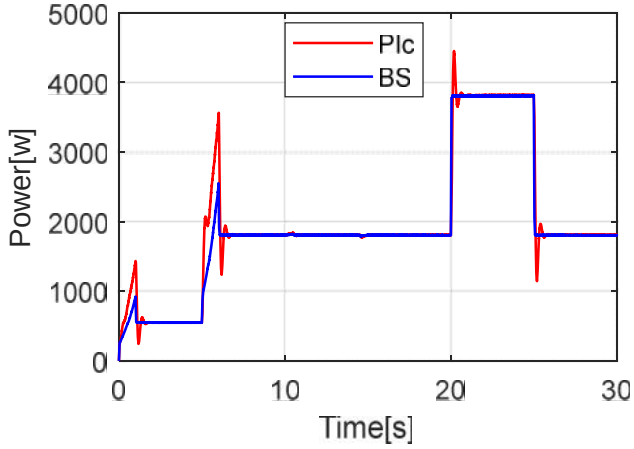

Fig.21. Battery power in different cases

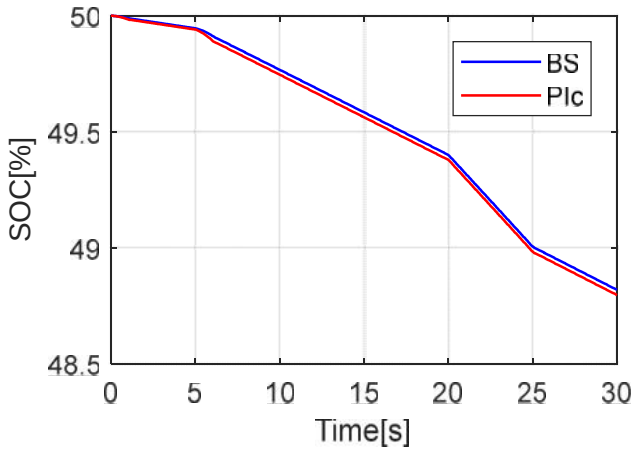

Fig.22. State of battery charge

Electric current increases when acceleration or when the scooter enters a slope road, causing an increase in energy consumption. However, it decreases more than usual in the case of battery charging.

Table 4. Variation of Battery current, battery power and SOC, in different trajectory phases.

Time [s]	**Battery current [A]**		**Consumed Battery Power [W]**		**SOC [%]**	
	PI	Backstepping	PI	Backstepping	PI	Backstepping
0	0	0	0	0	50.000	50.000
1	6.72	4.31	1432	921	49.98	49.99
6	17.03	12.06	3561	2551	49.89	49.91
20.18	21.68	18.44	4454	3815	49.37	49.39
25.17	5.5	8.69	1144	1805	48.97	49

The significant increase in overshooting in the PI leads to an increase in acceleration as well as the aerodynamic torque applied to the scooter, which leads to an increase in the battery power compared to the backstepping console, as shown in Table 4.

5. CONCLUSION

This study introduces an electric scooter design with a traction system consisting of two BLDC motor that propel the rear wheels. Both engines are independently controlled by a non-linear controller via backstepping method. Also, an electronic differential is used to ensure the security of passengers in urban transportation when the vehicle accesses a curved road. The system is modelled and traced the performance of the system under different speeds and as well as subjecting it to some disturbances according to the topography of a particular road. The used parameters of electric scooter, BLDCM and bidirectional buck-boost DC-DC converter are given in Table 5 and Table 6 on the Appendix section, respectively. The performance of the system whose speed is controlled by a non-linear backstepping controller is compared with a classical PI controller. The obtained results show the very fast response of the studied system during acceleration, entering a curved road or a sloping road as well as the high capacity of electronic differentials when the scooter enters a curved road.

Appendix

Table 5. The parameters of electric scooter, BLDCM and bidirectional Buck-Boost dc-dc converter

	Electric Scooter Parameters	
Symbol	**Parameter**	**Value**
r_w	Wheel radius	0.29m
η	Total transmission efficiency	93%
M_s	Scooter mass	230kg
S	Scooter frontal area	2.09 m^2
f_s	Scooter friction coefficient	0.01
L_w	Distance between the back and the front wheel	2.4m
d_w	Distance between two rear wheels	1.25m
	BLDC Motor Parameters	
R	Stator winding resistance	8.175 Ω
L	Stator leakage inductance	8.5 mH
f	Friction coefficient	0.001
P	Number of poles	4

Table 6. Parameters of the bidirectional Buck-Boost dc-dc converter

Bidirectional Buck-Boost Dc-Dc Converter Parameters	
Parameter	**Value**
Nominal baterry voltage	220V
Nominal DC link voltage	450V
DC link load resistance	300 Ω
Inductor	4.4mH
Capacitor	250µF
Switching frequency	20kHz

6. REFERENCES

[1] Hichem C., Nasri A., Kayisli K., "Fuzzy Logic Speed Control for Three-Wheel Electric Scooter", International Journal Of Renewable Energy Research (IJRER), 2019, Vol.9, No.3, pp.1443-1450.

[2] Hollingsworth J., Copeland B., Johnson J.X., "Are E-Scooters Polluters? The Environmental Impacts of Shared Dockless Electric Scooters", Environmental Research Letters, 2019, Vol.14, No.8, 084031.

[3] Zhang, Q. C., & Ma, R. Q. "Backstepping High Order Sliding Mode Control for Brushless DC Motor Speed Servo Control System", Control and Decision, 2016, Vol.6, No.31, pp.962-968.

[4] Hu, J. H., Zou, J. B., "Modeling and Simulation for Adaptive Backstepping Control of PMSM, Journal of System Simulation, 2007, Vol.19, pp.247-303.

[5] Hu, J., Dawson, D. M., Carroll, J. J., "An Adaptive Integrator Backstepping Tracking Controller for Brushless DC Motor/Robotic Load", IEEE American Control Conference-ACC'94, 1994, Vol.2, pp.1401-1405).

[6] Guo, Y., Ma, D., Wang, X., Le, G., "Application of Backstepping Control to AC Position Servo System", Machine Tool & Hydraulics, 2011, Vol.1, pp.1-17.

[7] Shu, A. N., "Application of Sliding Mode Control with Backstepping in BLDCM Servo System", 2008, Mechanical Engineering & Automation, Vol.6, pp.131-140.

[8] Shen, Y.X., Wu, D.H., Li, S.D., Ji, Z.C., "Backstepping Method Modeling for Position Servo Controller of Permanent Magnet Synchronous Motor", Acta Simulata Systematica Sinica, Vol.6,

pp.22-34.

[9] Lin, C.H., "Hybrid Recurrent Wavelet Neural Network Control of PMSM Servo-Drive System for Electric Scooter", International Journal of Control, Automation and Systems, 2014, Vol.12, No.1, pp.177-187.

[10] Chen, B.C., Wu, Y.Y., Wu, Y.L., Lin, C.C., "Adaptive Power Split Control for A Hybrid Electric Scooter, IEEE Transactions on Vehicular Technology, 2011, Vol.60, No.4, pp.1430-1437.

[11] Lin, C.H., "Novel adaptive recurrent Legendre neural network control for PMSM servo-drive electric scooter", Journal of Dynamic Systems, Measurement, and Control, 2015, Vol.137, No.1, 011010.

[12] Chen, B.C., Chu, C.H., Huang, S.J., "Fuzzy Sliding Mode Control of Traction Control System for Electric Scooter", IEEE Seventh International Conference on Fuzzy Systems and Knowledge Discovery, 2010, Vol. 2, pp.691-695.

[13] Chu, C.L., Tsai, M.C., Chen, H.Y., "Torque Control of Brushless DC Motors Applied to Electric Vehicles", IEEE IEMDC International Electric Machines and Drives Conference, 2001, Vol.1, pp.82-87.

[14] Tsai, C.C., Huang, H.C., Lin, S.C., "Adaptive Neural Network Control of A Self-Balancing Two-Wheeled Scooter". IEEE Transactions on Industrial Electronics, 2010, Vol.57, No.4, pp.1420-1428.

[15] Son, N.N., Anh, H.P.H., "Adaptive Backstepping Self-Balancing Control of A Two-Wheel Electric Scooter". International Journal of Advanced Robotic Systems, 2014, Vol.11, No.10, pp.1-11.

[16] Anh, H.P.H., Son, N.N., "Hybrid PD and Adaptive Backstepping Control for Self-Balancing Two-Wheel Electric Scooter", Journal of Computer Science and Cybernetics, 2014, Vol.30, No.4, 347-360.

[17] Kim, I.S, "Nonlinear State of Charge Estimator for Hybrid Electric Vehicle Battery", IEEE Transactions on Power Electronics, 2008, Vol.23, No.4, pp.2027-2034.

[18] Nasri A., Gasbaoui B., "Four Wheel Electric Vehicle Behavior using Fuel Cell Supply Moving on Mountain Region Condition", International Journal on Electrical Engineering and

Informatics, 2017, No.9, No.3, pp.469-481.

[19] Kayisli, K., Tuncer, S., Poyraz, M., "An Educational Tool for Fundamental DC–DC Converter Circuits and Active Power Factor Correction Applications", Computer Applications in Engineering Education, Vol.21, No.1, pp.113-134.

[20] Hemati, N., "Strange Attractors in Brushless DC Motors". IEEE Transactions on Circuits and Systems I: Fundamental Theory and Applications, 1994, Vol.41, No.1, pp.40-45.

[21] Qi, G., "Energy Cycle of Brushless DC Motor Chaotic System", Applied Mathematical Modelling, 2017, Vol.51, pp.686-697.

[22] Cai-Xue, C., Yun-Xiang, X., Yong-Hong, L., "Backstepping Control of Speed Sensorless Permanent Magnet Synchronous Motor based on Slide Model Observer", International Journal of Automation and Computing, 2015, Vol.12, No.2, pp.149-155.

[23] Premkumar, K., Manikandan, B. V., & Kumar, C. A. "Antlion algorithm optimized fuzzy PID supervised on-line recurrent fuzzy neural network based controller for brushless DC motor", Electric Power Components and Systems, 2017, Vol.45, No.20, pp.2304-2317.

How to cite this article:
Chergui H, Abdelfatah N, Korhan K. Non-Linear Backstepping Speed Control for Asian Electric Scooter Uses. Fundam. Appl. Sci., 2021, *13(1), 400-423.*